Light emission characteristics of nonpolar *a*-plane GaN-based photonic crystal defect cavities

Tsung Sheng Kao[1], Tzeng-Tsong Wu[1], Che-Wei Tsao[1], Jyun-Hao Lin[2], Da-Wei Lin[1], Shyh-Jer Huang[3], Tien-Chang Lu[*,1], Hao-Chung Kuo[1], Shing-Chung Wang[1], and Yan-Kuin Su[2,4]

[1]Department of Photonics & Institute of Electro-Optical Engineering, National Chiao Tung University, Hsinchu 300, Taiwan
[2]Institute of Microelectronics, Department of Electrical Engineering, Advanced Optoelectronic Technology Center, National Cheng Kung University, Tainan 701, Taiwan
[3]Department of Electrical Engineering, University of California, Los Angeles, USA
[4]Department of Electrical Engineering, Kun-Shan University, Tainan 710, Taiwan
* timtclu@mail.nctu.edu.tw

ABSTRACT

In this paper, nonpolar *a*-plane GaN-based photonic crystals (PCs) with different defect cavities have been demonstrated. By using a micro-photoluminescence (μ-PL) system operated at 77 K, the dominant resonant modes of the GaN-based PC defect cavities show high quality factor (Q) values in the light emission performance which can be up to 4.3×10^3. Moreover, the degree of polarization (DOP) of the light emission from the nonpolar GaN-based PC defect cavities was measured to achieve around 64 % along the *m* crystalline direction.

Keywords- GaN, nonpolar, *a*-plane, photonic crystal, defect cavity.

1. INTRODUCTION

Photonic crystals (PCs) with defect cavities have been widely investigated and applied in advanced lasing devices owing to their significant photonic bandgap effect, which can be sufficiently employed to realize the photon confinement in a small mode volume and light emission with high quality factor (Q) values [1-4]. By changing the defect cavity parameters such as the cavity types, radius of constituent nanoholes, lattice constants, and the material compositions with different refractive indices, specific light emission characteristics could be acquired and employed in many applications such as the ultra-low threshold lasers and photonic integrated circuits [5-13].

Among the great efforts made previously in the development of PC defect cavity lasers, most the studies were reported using GaAs and InP-based materials because the suspended thin membrane structures which are beneficial to achieve high Q values can be easily made by selective chemical etching to remove the underneath sacrificial layer [1,2]. However, some unwanted damages and composites cannot be avoided during the reaction process. Recently, GaN-based materials have attracted much attention and been considered as a competitive material for exploring next-generation optoelectronic devices. GaN-based materials exhibit many promising properties such as high exciton binding energy and oscillator strength which is beneficial for supporting high efficiency light emission and exciton-photon coupling capabilities. However, the PC defect cavity lasers based on the use of GaN-based materials were seldom addressed because of the relative challenging etching process in the thin membrane structures fabrications. Several feasible methods have been proposed such as the photo-electro-chemical (PEC) etching of InGaN sacrificial layers [14-17], selective chemical wet-etching of InGaN layers grown on Si substrate [18,19] and selective thermal decomposition of GaN layers [20]. Nevertheless, it is still a challenge to fabricate GaN-based membrane structures due to the complex etching process of particular epitaxial structures.

Although the fabrication of a thin membrane structure is relatively difficult in the GaN-based system, the quest to demonstrate a GaN-based PC defect nanocavity laser is still fascinating, especially for the nonpolar GaN-based materials. The main characteristic of nonpolar GaN is free of polarization fields in the quantum wells which can lead to high internal quantum efficiency and fabrication flexibility [21-26]. Furthermore, nonpolar GaN-based materials can exhibit the anisotropic gain in the *m*-axis or *a*-axis which is beneficial for development of low threshold and high power lasers [27-29].

High Contrast Metastructures IV, edited by Connie J. Chang-Hasnain, David Fattal, Fumio Koyama, Weimin Zhou, Proc. of SPIE Vol. 9372, 93720C · © 2015 SPIE
CCC code: 0277-786X/15/$18 · doi: 10.1117/12.2078577

In this letter, the nonpolar *a*-plane GaN-based photonic crystals with different defect nano-cavities have been fabricated. The patterns were defined by an e-beam lithography (EBL) system and the thin membrane structures of the PC defect cavities were fabricated by using the focused ion beam (FIB) milling technique [30-32]. Via a micro-photoluminescence (μ-PL) system operated at 77 K, the light emission from the PC defect cavities has been characterized and demonstrated with high Q values in the light emission performance. Finally, the numerical calculation results were in a good agreement with the experimental results.

2. SIMULATION

The layer structure of the nonpolar *a*-plane GaN-based photonic crystals with defect cavities is schematically shown in Fig. 1(a), while the corresponding patterns of hexagonal H2 and linear L7 defect cavities which were performed in the simulations are represented Fig. 1(b). Numerical simulations were carried out with the three-dimensional (3D) finite difference time domain (FDTD) method and the simulation parameters such as the radius (*r*) of nanoholes, lattice constant (*a*) and the thin membrane thicknesses were extracted from the real devices. In the simulation model, the direction of *a*-plane PC L7 cavities was designed to parallel the *c*-axis. Also, according to the work done by E. Matioli, *et. al*. [33], the quantum mechanical dipole moments are well described by electric oscillating dipole moments from classic electromagnetism, radiating an electric field $\vec{E}$ mostly parallel to the *m* direction for the *a*-plane GaN. Therefore, electric dipoles were placed in the *m*-axis direction to represent the sample grown on the *a*-plane GaN as it indicated at the bottom of Fig. 1(b).

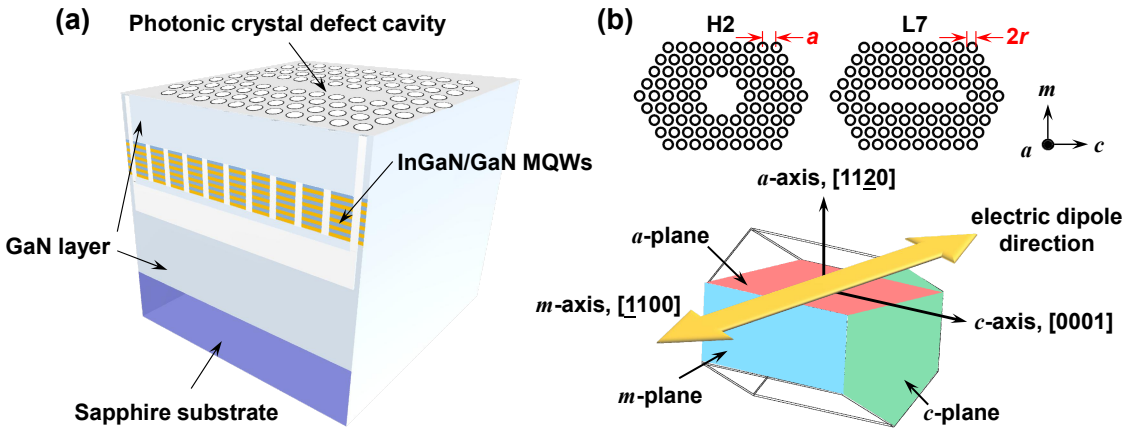

Figure 1 Schematic diagram of the nonpolar GaN-based PC defect cavities. (a) The layer structure of the nonpolar GaN-based PC defect cavities. (b) The corresponding patterns of hexagonal H2 and linear L7 defect cavities performed in the FDTD simulations. The simulation parameters such as the lattice constants (*a*) and the radius (*r*) of constituent nanoholes were extracted from the real sample devices.

3. EXPERIMENT

The nonpolar *a*-plane GaN-based structures were epitaxially grown on a *r*-plane sapphire substrate via the metal-organic chemical vapor deposition (MOCVD) method, including a six pair InGaN/GaN multiple quantum wells (MQWs) layer of about 60 nm sandwiched between a 2 μm- and a 30 nm-thick un-doped GaN layers as the schematic fabrication process flow represented in Fig. 2(a). To etch the photonic crystal patterns with defect cavities onto the above GaN-based structures, a 200 nm-thick SiN_x dielectric layer was first deposited on the top of the grown GaN-based samples as a hard mask using a plasma-enhanced chemical vapor deposition (PECVD) system and followed by a spin-coated poly-methyl methacrylate (PMMA) photoresist layer. Subsequently, the photonic crystal patterns with required defect cavities were defined by the electron-beam lithography (EBL) method, transferred to the SiN_x hard mask and etched through the GaN and MQWs layers using reactive-ion etching (RIE) and the induced-coupled plasma (ICP) methods, respectively. At the end of the fabrication process, the focused-ion beam (FIB) milling was utilized by tilting the samples to fabricate the thin

membrane structure at the bottom of the GaN-based photonic crystal defect cavities, generating a free-standing-like thin film with a large air-gap as indicated in Fig. 2(h).

Figures 3(a) and 3(b) show the scanning electron microscope (SEM) images of the patterned nonpolar *a*-plane GaN-based PC with a hexagonal H2 and a linear L7 defect cavities, respectively. The radius (*r*) of constituent nanoholes and the lattice constant (*a*) in the PC H2 defect cavity were measured to be 26.5 nm and 105 nm, giving the r/a ratio of the photonic crystal is around 0.257. For the sample parameters extracted in the nonpolar GaN-based PC L7 defect cavity, the radius and lattice constant are 29 nm and 122 nm, respectively. Figure 3(c) shows the membrane area of the nonpolar GaN layer in a tilted angle view. The whole membrane area is estimated to be 10 μm^2. As an enlarged image shows in Fig. 3(d), the thickness of the cleaved thin membrane layer is about 235 nm.

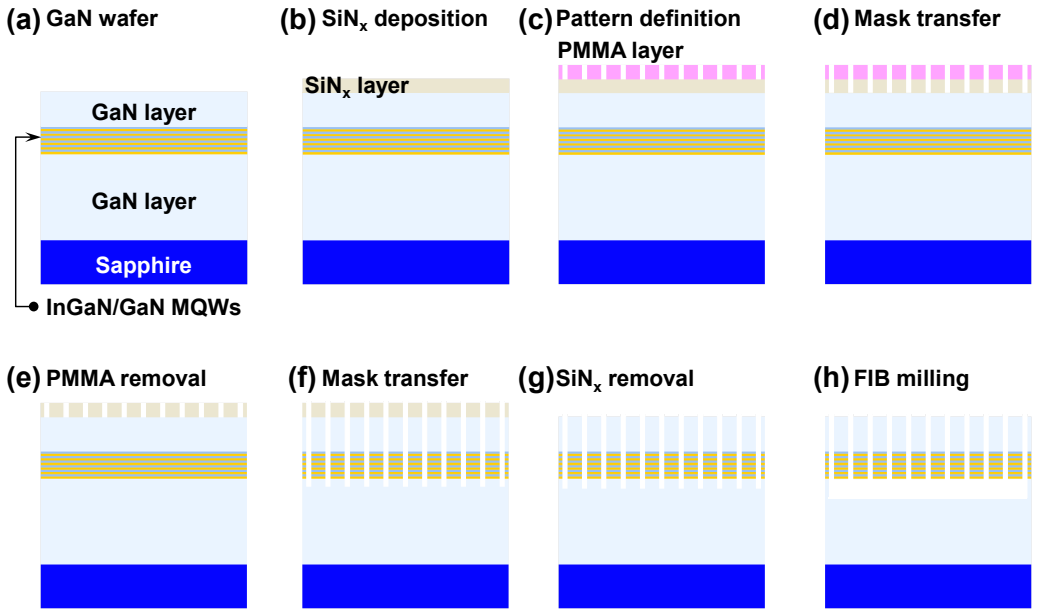

Figure 2 Fabrication process flow for the nonpolar *a*-plane GaN-based PC defect cavities. Via the above fabrication process, the nonpolar *a*-plane GaN-based PC with designed defect cavities can be accomplished. By the FIB milling technique, the thin membrane structure of the PC defect cavity can be obtained to achieve high Q value in light emission performance.

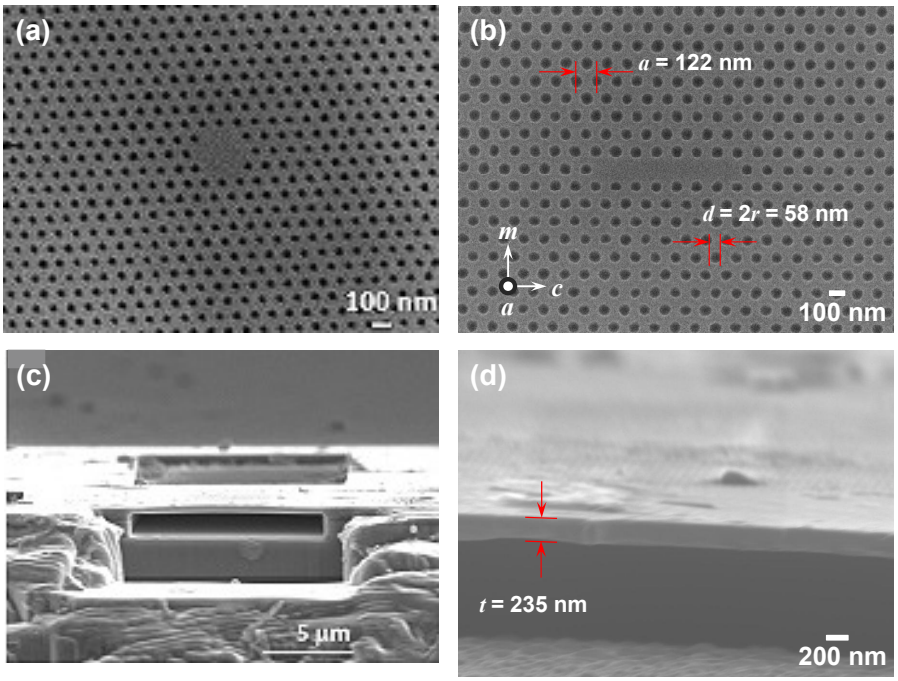

Figure 3 SEM images of the fabricated nonpolar *a*-plane GaN-based PC defect cavities. The SEM images of nonpolar GaN-based PCs with (a) hexagonal H2 and (b) linear L7 defect cavities. (c) and (d) are the titled angle views of the nonpolar GaN membrane layer. The whole area and the thickness of the membrane thin film is about 10 μm^2 and 235 nm, respectively.

To investigate the light emission properties of the fabricated GaN-based nonpolar PC with defect cavities, the micro-photoluminescence (μ-PL) measurements were conducted at 77 K using a 325 nm He-Cd continuous wave (CW) laser as an optical pumping source in the measurement system. The laser beam was normally incident onto the devices with a spot size of around 15 μm in diameter, covering the whole photonic crystal patterns. The reflected μ-PL emission signal was collected by a 15X objective lens normal to the sample surface, then passed through a multiple mode fiber with a 600μm core and fed into a charge-couple device (Jobin-Yvon iHR320 spectrometer). The spectral resolution was about 0.07 nm for spectral measurements.

4. RESULTS AND DISCUSSIONS

Figures 4(a) and 4(b) reveal the μ-PL emission spectra of the nonpolar *a*-plane GaN-based photonic crystals with hexagonal H2 and linear L7 defect cavities, respectively. The dominated resonant mode is found about 388 nm for the PC H2 defect cavity, while located at around 419 nm for the PC L7 device. The locations of these two resonant modes are correspondent with the *r*/*a* ratio and still occurred in the photonic band gap range. To estimate the Q values of the resonant modes, we performed the Lorentz fitting on the measured data sets and represented the fitting results as the red curves shown in the figures. The light emission characteristics of the nonpolar *a*-plane GaN-based PC H2 and L7 defect cavities are estimated to be 4300 and 2000, respectively. The high Q factor in the nonpolar GaN PC defect cavities indicates good optical confinement provided by photonic bandgap in the lateral direction and total internal reflection in the vertical direction. Moreover, the Q values of our nonpolar GaN PC defect cavities are comparable to the previous studies of PC defect cavities grown on *c*-plane GaN, demonstrating that the FIB milling technique is capable to create the smooth surface of the thin membrane layer. In order to confirm the resonant modes observed in the photonic crystals with defect cavities, a series of numerical analyses was conducted as described above. The results are shown in Fig. 4(c) and 4(d) for the photonic crystals with H2 and L7 defect cavities respectively, showing that the calculated resonant wavelengths are located at 380 nm and 412 nm. The results are correspondent with the one obtained in experiments.

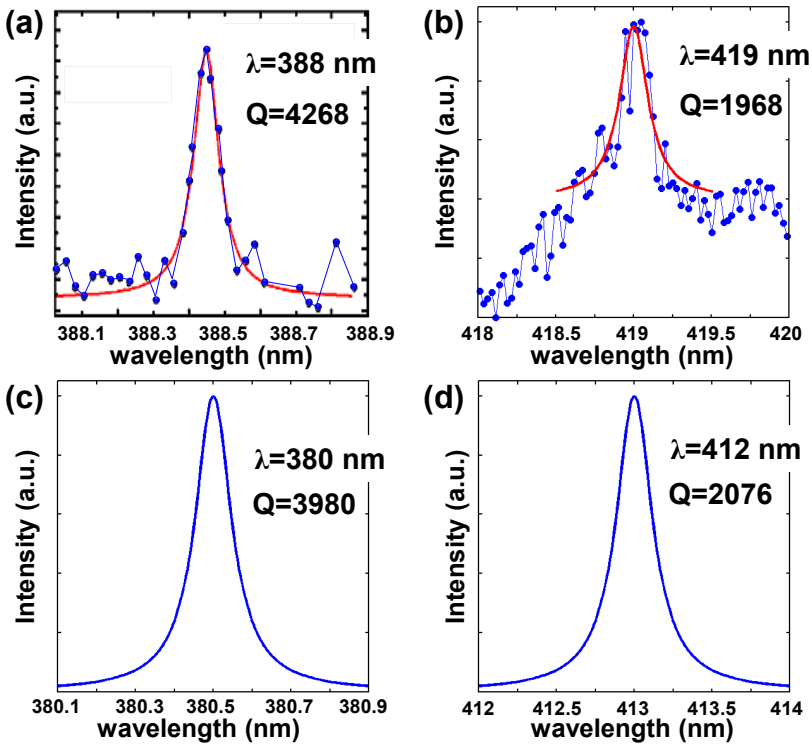

Figure 4 Resonant modes of the nonpolar *a*-plane GaN-based PC defect cavities. (a) and (b) show the measured PL results of the nonpolar a-plane GaN-based PC with H2 and L7 defect cavities, respectively. (c) and (d) represent the corresponding simulation results of the two types of PC defect cavities.

Figures 5(a) and 5(b) show the polarization characteristics of the nonopolar *a*-plane GaN-based photonic crystals with H2 and L7 defect cavities, respectively. The degree of polarization (DOP) is defined as $(I_{max}-I_{min})/(I_{max}+I_{min})$, where the I_{max} and I_{min} are the maximum and the minimum intensity of the resonant mode peak. The measured DOP was calculated to be 64 % for the PC H2 defect cavity and 52 % for the PC L7 device. In order to understand the enhanced DOP value in the PC cavities, theoretical simulations were conducted to calculate the mode pattern at the corresponding resonant wavelengths as shown in Fig. 5(c) and 5(d). Both the figures show the square of electric field patterns in the nonpolar GaN PC cavities. They can be observed that the electric fields are oscillating along the *m*-axis. The high DOP value of the nonpolar GaN PC cavities could be attributed to the specific electric field distribution along the *m*-axis enhancing the dipole oscillation.

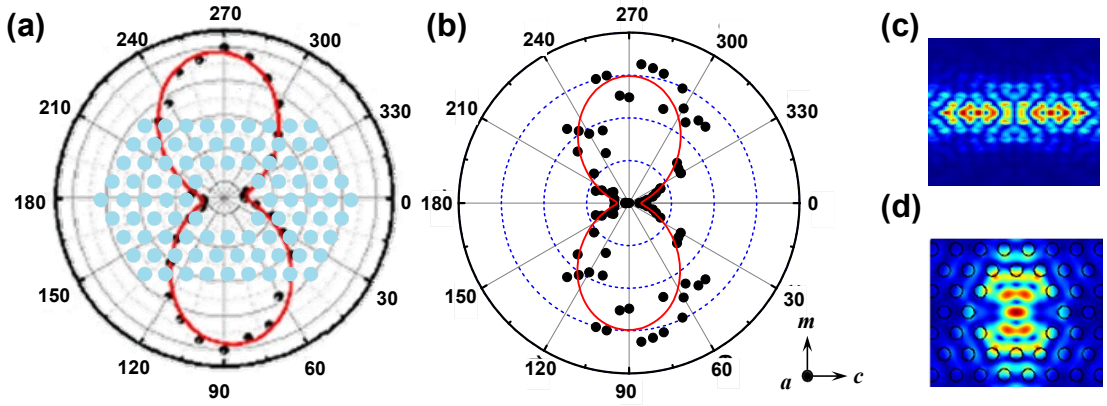

Figure 5 The polar plot of the resonant peak intensities for the nonpolar *a*-plane GaN-based PC defect cavities. (a) and (b) show the DOP performance of the nonpolar a-plane GaN-based PC H2 and L7 defect cavities, respectively. (c) and (d) represent the simulation results of the corresponding electric field distribution on the surface of the defect cavity devices.

5. CONCLUSION

In conclusion, the light emission characteristics between the nonopolar *a*-plane GaN-based photonic crystals with hexagonal H2 and linear L7 defect cavities have been demonstrated and analyzed. The μ-PL emission spectra indicated that dominated resonant modes of each PC defect cavity device occurred at 388 nm and 419 nm at 77 K. Q values of the corresponding resonant modes in the nonpolar *a*-plane GaN-based PC H2 and PC L7 defect cavities were estimated to be 4.3×10^3 and 2×10^3, respectively. Moreover, the DOP values of the nonpolar *a*-plane GaN PC H2 and L7 defect cavities were estimated to be 64 % and 52 %, which were both higher than that of the *c*-plane GaN device. It suggests that the nonpolar *a*-plane GaN-based PC with defect cavities can be potential for the development of high quality and high efficiency optoelectronic devices.

ACKNOWLEDGMENT

This work was supported in part by the Ministry of Education Aim for the Top University program and by the National Science Council of Taiwan under Contract No. NSC99-2622-E009-009-CC3 and NSC98-2923-E-009-001-MY3.

REFERENCES

[1] Park, H. G., Kim, S. H., Kwon, S. H., Ju, Y., Yang, J. K., Baek, J. H., Kim, S. B., and Lee, Y. H., "Electrically driven single-cell photonic crystal laser", *Science* **305** 1444 (2004).

[2] Painter, O., Lee, R., Scherer, A., Yariv, A., O'brien, J., Dapkus, P., and Kim, I., "Two-dimensional photonic band-gap defect mode laser", *Science* **284** 1819 (1999).

[3] John, S., "Strong localization of photons in certain disordered dielectric superlattices", *Phys. Rev. Lett.* **58** 2486 (1987).

[4] Yablonovitch, E., "Inhibited spontaneous emission in solid-state physics and electronics", *Phys. Rev. Lett.* **58** 2059 (1987).

[5] Meier, M., Mekis, A., Dodabalapur, A., Timko, A., Slusher, R. E., Joannopoulos, J. D., and Nalamasu, O., "Laser action from two-dimensional distributed feedback in photonic crystals", *Appl. Phys. Lett.* **74** 7 (1999).

[6] Lu, T. C., Chen, S. W., Lin, L. F., Kao, T. T., Kao, C. C., Yu, P., Kuo, H. C., Wang, S. C., and Fan, S. H., "GaN-based two-dimensional surface-emitting photonic crystal lasers with AlN/GaN distributed bragg reflector", *Appl. Phys. Lett.* **92** 011129 (2008).

[7] Matsubara, H., Yoshimoto, S., Saito, H., Jianglin, Y., Tanaka, Y., and Noda, S., "GaN photonic-crystal surface-emitting laser at blue-violet wavelengths", *Science* **319** 445 (2008).

[8] Kawashima, S., Kawashima, T., Nagatomo, Y., Hori, Y., Iwase, H., Uchida, T., Hoshino, K., Numata, A., and Uchida, M., "GaN-based surface-emitting laser with two-dimensional photonic crystal acting as distributed-feedback grating and optical cladding", *Appl. Phys. Lett.* **97** 251112 (2010).

[9] Matioli, E., Rangel, E., Iza, M., Fleury, B., Pfaff, N., Speck, J., Hu, E., and Weisbuch, C., "High extraction efficiency light-emitting diodes based on embedded air-gap photonic-crystals", *Appl. Phys. Lett.* **96** 031108 (2010).

[10] Imada, M., Chutinan, A., Noda, S., and Mochizuki, M., "Multidirectionally distributed feedback photonic crystal lasers", *Phys. Rev. B* **65** 195306 (2002).

[11] Yokoyama, M., and Noda, S., "Polarization mode control of two-dimensional photonic crystal laser having a square lattice structure", *IEEE J. Quantum Electron.* **39** 1074 (2003).

[12] Kim, M., Kim, C. S., Bewley, W. W., Lindle, J. R., Canedy, C. L., Vurgaftman, I., and Meyer, J. R., "Surface-emitting photonic-crystal distributed-feedback laser for the midinfrared", *Appl. Phys. Lett.* **88** 191105 (2006).

[13] Sirigu, L., Terazzi, R., Amanti, M. I., Giovannini, M., Faist, J., Dunbar, L. A., and Houdré, R., "Terahertz quantum cascade lasers based on two-dimensional photonic crystal resonators", *Opt. Exp.* **16** 5206 (2008)

[14] Arita, M., Ishida, S., Kako, S., Iwamoto, S., and Arakawa, Y., "AlN air-bridge photonic crystal nanocavities demonstrating high quality factor", *Appl. Phys. Lett.* **91** 051106 (2007).

[15] Kim, D. U., Kim, S., Lee, J., Jeon, S. R., and Jeon, H., "Free-standing GaN-based photonic crystal band-edge laser", *IEEE Photon. Technol. Lett.* **23** 1454 (2011).

[16] Choi, Y. S., Hennessy, K., Sharma, R., Haberer, E., Gao, Y., DenBaars, S. P., Nakamura, S., Hu, E. L., and Meier, C., "GaN blue photonic crystal membrane nanocavities", *Appl. Phys. Lett.* **87** 243101 (2005)

[17] Lin, C. H., Wang, J. Y., Chen, C. Y., Shen, K. C., Yeh, D. M., Kiang, Y. W., and Yang, C., "A GaN photonic crystal membrane laser", *Nanotech.* **22** 025201 (2011)

[18] Neel, D., Sergent, S., Mexis, M., Sam Giao, D., Guillet, T., Brimont, C., Bretagnon, T., Semond, F., Gayral, B., David, S., Checoury, X., and Boucaud, P., "AlN photonic crystal nanocavities realized by epitaxial conformal growth on nanopatterned silicon substrate", *Appl. Phys. Lett.* **98** 261106 (2011)

[19] Trivino, N. V., Rossbach, G., Dharanipathy, U., Levrat, J., Castiglia, A., Carlin, J. F., Atlasov, K. A., Butte, R., Houdre, R., and Grandjean, N., "High quality factor two dimensional GaN photonic crystal cavity membranes grown on silicon substrate", *Appl. Phys. Lett.* **100** 071103 (2012)

[20] Arita, M., Kako, S., Iwamoto, S., and Arakawa, Y., "Fabrication of AlGaN two-dimensional photonic crystal nanocavities by selective thermal decomposition of GaN", *Appl. Phys. Exp.* **5** 126502 (2012)

[21] Craven, M., Lim, S. H., Wu, F., Speck, J. S., and DenBaars, S. P., "Structural characterization of nonpolar (11$\bar{2}$0) a-plane GaN thin films grown on (1$\bar{1}$02) r-plane sapphire", *Appl. Phys. Lett.* **81** 469 (2002).

[22] Haskell, B., Wu, F., Matsuda, S., Craven, M. D., Fini, P. T., Denbaars, S. P., Speck, J. S., and Nakamura, S., "Structural and morphological characteristics of planar (11$\bar{2}$0) a-plane gallium nitride grown by hydride vapor phase epitaxy", *Appl. Phys. Lett.* **83** 1554 (2003).

[23] Waltereit, P., Brandt, O., Ramsteiner, M., Trampert, A., Grahn, H. T., Menniger, J., Reiche, M., Uecker, R., Reiche, P., and Ploog, K. H., "Growth of m-plane GaN(11-00): A way to evade electrical polarization in nitrides", *Phys. Status. Solidi A* **180** 133 (2000).

[24] Holder, C., Speck, J. S., DenBaars, S. P., Nakamura, S., and Feezell, D., "Demonstration of nonpolar GaN-based vertical-cavity surface-emitting lasers", *Appl. Phys. Exp.* **5** 092104 (2012).

[25] Waltereit, P., Brandt, O., Ramsteiner, M., Trampert, A., Grahn, H. T., Menniger, J., Reiche, M., Uecker, R., Reiche, P., and Ploog, K. H., "Nitride semiconductors free of electrostatic fields for efficient white light-emitting diodes", *Nature* **406** 865 (2000).

[26] Chang, C. Y., Huang, H. M., Lai, C. M., and Lu, T. C., "Characteristics of polarized light emission in *a*-plane GaN-based multiple quantum wells", *IEEE J. Quantum Electron.* **48** 867 (2012).

[27] Ohtoshi, T., Niwa, A., and Kuroda, T., "Dependence of optical gain on crystal orientation in wurtzite–GaN strained quantum-well lasers", *J. Appl. Phys.* **82** 1518 (1997).

[28] Scheibenzuber, W., Schwarz, U., Veprek, R., Witzigmann, B., and Hangleiter, A., "Calculation of optical eigenmodes and gain in semipolar and nonpolar InGaN/GaN laser diodes", *Phys. Rev. B* **80** 115320 (2009).

[29] Takigawa, S., and Noda, S., "Analysis of two-dimensional photonic crystal with anisotropic gain", *Opt. Exp.* **19** 9475 (2011).

[30] Babinec, T. M., Choy, J. T., Smith, K. J. M., Khan, M., and Loncar, M., "Design and focused ion beam fabrication of single crystal diamond nanobeam cavities", *J. Vac. Sci. Technol. B* **29** 010601 (2011).

[31] Wu, T. T., Syu, Y. C., Wu, S. H., Chen, W. T., Lu, T. C., Wang, S. C., Chiang, H. P., and Tsai, D. P., "Sub-wavelength GaN-based membrane high contrast grating reflectors", *Opt. Exp.* **20** 20551 (2012).

[32] Wu, T. T., Lo, S. Y., Huang, H. M., Tsao, C. W., Lu, T. C., and Wang, S. C., "High quality factor nonpolar GaN photonic crystal nanocavities", *Appl. Phys. Lett.* **102** 191116 (2013).

[33] Matioli, E., Brinkley, S., Kelchner, K. M., Hu, Y. -L., Nakamura, S. DenBaars, S., Speck, J., and Weisbuch, C., "High-brightness polarized light-emitting diodes", *Light: Appl.. & Sci.* **1** e22 (2012).